Molecular Biology of the Cell
Vol. 19, 2014–2025, May 2008

# Neuronal Death by Oxidative Stress Involves Activation of FOXO3 through a Two-Arm Pathway That Activates Stress Kinases and Attenuates Insulin-like Growth Factor I Signaling

**David Dávila and Ignacio Torres-Aleman**

Laboratory of Neuroendocrinology, Cajal Institute, Consejo Superior de Investigaciones Cientificas (CSIC); Centro de Investigación Biomédica en Red sobre Enfermedades Neurodegenerativas (CIBERNED), Madrid, Spain

Submitted August 21, 2007; Revised January 28, 2008; Accepted February 7, 2008
Monitoring Editor: Donald Newmeyer

**Oxidative stress kills neurons by stimulating FOXO3, a transcription factor whose activity is inhibited by insulin-like growth factor I (IGF-I), a wide-spectrum neurotrophic signal. Because recent evidence has shown that oxidative stress blocks neuroprotection by IGF-I, we examined whether attenuation of IGF-I signaling is linked to neuronal death by oxidative stress, as both events may contribute to neurodegeneration. We observed that in neurons, activation of FOXO3 by a burst of oxidative stress elicited by 50 $\mu$M hydrogen peroxide ($H_2O_2$) recruited a two-pronged pathway. A first, rapid arm attenuated AKT inhibition of FOXO3 through p38 MAPK-mediated blockade of IGF-I stimulation of AKT. A second delayed arm involved activation of FOXO3 by Jun-kinase 2 (JNK2). Notably, blockade of IGF-I signaling through p38 MAPK was necessary for JNK2 to activate FOXO3, unveiling a competitive regulatory interplay between the two arms onto FOXO3 activity. Therefore, an abrupt rise in oxidative stress activates p38 MAPK to tilt the balance in a competitive AKT/JNK2 regulation of FOXO3 toward its activation, eventually leading to neuronal death. In view of previous observations linking attenuation of IGF-I signaling to other causes of neuronal death, these findings suggest that blockade of trophic input is a common step in neuronal death.**

## INTRODUCTION

Cell metabolism generates potentially harmful reactive oxygen species (ROS). At moderate levels, ROS act as second messengers in different cellular functions (Droge, 2002). At the same time a variety of mechanisms protects cells against excess ROS. Therefore, low chronic bursts of free radicals are probably not detrimental to cell physiology (Finkel, 2003). However, chronic and/or abrupt increases in ROS levels above a physiological threshold may trigger cell death by interfering with normal cellular operations. Indeed, oxidative stress is putatively involved in many neurodegenerative diseases, such as Alzheimer's dementia or amyotrophic lateral sclerosis (Behl *et al.*, 1994; Wu *et al.*, 2006). This likely relates to the observation that neurons are particularly vulnerable to increases in ROS levels, because these cells have a reduced capacity to detoxify ROS (Dringen *et al.*, 2005). Furthermore, it is well established that oxidative stress is involved in the aging process (Droge, 2003), which in turn likely contributes to the link between neurodegenerative diseases and old age probably due to progressive neuronal attrition. Therefore, the study of the pathways that transform normal cellular constituents such as ROS (Droge, 2002) into death effectors constitutes an important aspect of current research in neuroprotection.

Insulin-like growth factor I (IGF-I), a prototype neuron survival factor (Torres-Aleman, 2005) activates IGF-I receptors that recruit and phosphorylate IRS docking proteins that activate phosphatidyl inositol 3 kinase (PI3K). In turn, PI3K activates the Ser/Thr-kinase B/AKT (Dudek *et al.*, 1997), which phosphorylates and inactivates transcription factors of the FOXO family (Biggs *et al.*, 1999; Brunet *et al.*, 1999). FOXO transcription factors are key players in cell death/life pathways. In neurons, FOXO has been involved mostly in cell death processes such as after trophic deprivation (Gilley *et al.*, 2003) or excess ROS (Lehtinen *et al.*, 2006). The presence of IGF-I in many types of brain injuries makes this peptide a likely participant in reactive responses to damage (Torres-Aleman, 2005). Indeed, IGF-I protects against neuronal insults (Trejo *et al.*, 2004) and is required for recovery after injury (Fernandez *et al.*, 1999). However, under experimental conditions recreating oxidative stress, IGF-I neuroprotection fails (Wu *et al.*, 2006; Zhong and Lee, 2007). In this context, ROS were reported to inactivate IGF-I receptor function through abnormal glycation (Wu *et al.*, 2006). This process could reflect a nonspecific generalized protein oxidation after prolonged exposure to ROS (Wu *et al.*, 2006).

However, IGF-I signaling is probably targeted by ROS in a more specific way. Thus, several mediators of the IGF-I/

This article was published online ahead of print in *MBC in Press* (http://www.molbiolcell.org/cgi/doi/10.1091/mbc.E07–08–0811) on February 20, 2008.

Address correspondence to: Ignacio Torres-Aleman (torres@cajal.csic.es).

Abbreviations used: $H_2O_2$, hydrogen peroxide; IGF-I, insulin-like growth factor I; JNK2, Jun-kinase 2; LDH, lactate dehydrogenase; PI, propidium iodide; PI3K, phosphatidyl inositol 3 kinase; ROS, reactive oxygen species.

insulin signaling cascade are modulated by redox state under physiological conditions (Lee *et al.*, 2002; Leslie, 2006). IGF-I likely modulates the generation of ROS by neurons through regulation of neuronal metabolism (Sonntag *et al.*, 2006). Additional support for this possibility is that ROS specifically interferes with insulin signaling at different steps (Hansen *et al.*, 1999; Houstis *et al.*, 2006), and insulin and IGF-I share the same or very similar intracellular pathways. Because the IGF-IR/AKT pathway is a wide-spectrum neuroprotective route, its attenuation may be involved in cell death by oxidative stress. In the present work we have explored this possibility in detail. We have found that oxidative stress elicits neuronal death through activation of FOXO by a dual process that involves timed activation of stress kinases and abrogation of IGF-I neuroprotection.

## MATERIALS AND METHODS

### *Animals and Reagents*

Postnatal day 7 Wistar rat pups (Harlan Labs, Barcelona, Spain) were used. All efforts were made to minimize suffering and reduce the number of animals. Animals were kept under light/dark conditions following EU guidelines (directive 86/609/EEC) and handled according to institutionally approved procedures. Antibodies to phospho-AKT ($Ser^{473}$), Jun kinases (JNKs), phospho-c-jun ($Ser^{63}$), phospho-p38MAPK ($Thr^{180}/Tyr^{182}$), p38MAPK, phospho-AMPK ($Thr^{172}$), AMPK, and mTOR inhibitor rapamycin were from Cell Signaling (Danvers, CT). Antibodies to 14-3-3 (K19), HA (F-7), phospho-JNKs ($Thr^{183}/Tyr^{185}$)(G7), IGF-I receptor (C-20), Bim (H-191), and AKT1/2 (H-136) were obtained from Santa Cruz Biotechnology (Santa Cruz, CA). Antibodies to IRS-1, phospho-IRS-1 ($Tyr^{612}$), and phospho-IRS-1 ($Ser^{312}$) were from Ab-Cam (Cambridge, United Kingdom). Antibodies to phospho-FOXO3 ($Thr^{32}$), phospho-FOXO3 ($SER^{253}$), FOXO3, $p^{85}$PI3K, and Neu-N were from Upstate Biotechnology (Billerica, MA). Antibody to MnSOD was obtained from Stressgen (San Diego, CA). Drug inhibitors against p38 mitogen-activated protein kinase (MAPK): SB239063 and PD169316, the JNKs inhibitor SP600125, the phosphatases PP2a and PP1 inhibitor okadaic acid, and protein kinase C inhibitors: bisindolylmaleimide, RO-31-8425, and Gö 6983 were all obtained from Calbiochem (San Diego, CA). Antibody against $\beta$-actin, the AMPK activator 5-iodo-tubercidin and $H_2O_2$ were purchased from Sigma (Steinheim, Germany).

### *Plasmids*

pECE-FOXO3 and pECE-FOXO3-TM (triple mutant T32A/S253A/S315A, herein called MFOXO3) were kindly provided by M. E. Greenberg (Harvard Medical School, Boston, MA). p6xDBE-luc (reporter luciferase plasmid with six copies of the DAF16 family protein-binding element) and pRL-TK (TK-Renilla luciferase) were a kind gift of B. M. Burgering (University Medical Centre, Utrecht, The Netherlands). Bim promoter luciferase construct was generously provided by P. Bouillet (Institute of Medical Research, Melbourne, Australia). Dominant negative FOXO3 (DN-FOXO3) was generated as described (Gilley *et al.*, 2003). DN-FOXO3 with a FLAG-tagged N-terminus was generated by PCR amplification of the DNA-binding domain (DBD; amino acids 141–268) of pECE-FOXO3a-TM using primers: 5′-ACTCGATCCGCTGGGGGCTCCGGGCAGCCG-3′ and 5′-actgaattcctagggtgcgcggccacggctc-3′ followed by cloning into BamHI- and EcoRI-restricted pCMV-flag. pCDNA3-AKT-CA (constitutively active AKT) was kindly provided by S. Pons (Biomedicine Institute, CSIC, Barcelona, Spain). pCDNA3-JIP (c-Jun N-terminal Kinase-interacting protein 1) was gently provided by M. Dickens (University of Leicester, United Kingdom), pCEV-MEKK was obtained through the generosity of M. J. Marinissen (Instituto de Investigaciones Biomédicas, CSIC, Madrid, Spain). pcDNA3-p38$\alpha$ agf (dominant negative [DN] p38$\alpha$) was generously given by J. D. Li (University of Rochester, New York), pcDNA3-p38$\beta$ agf (DN p38$\beta$) was kindly provided by R. J. Davis (Howard Hughes Medical Institute).

### *Cell Culture and Transfection*

Cerebellar granule cultures were produced from P7 rat cerebella as described previously (Garcia-Galloway *et al.*, 2003). In brief, cells were plated onto 6- or 12-well dishes coated with poly-L-lysine (1 $\mu$g/ml) at a respective final density of $1.5 \times 10^6$/well or $0.45 \times 10^6$/well. Cells were incubated at 37°C with 5% $CO_2$ in Neurobasal (Invitrogen, Carlsbad, CA) medium supplemented with 10% B27 (Invitrogen), glutamine (5 mM) and KCl (25 mM). All experiments were carried out with 3–7-d-old cultures, with neurons showing well developed neurite extensions. Granule neurons were transfected 24 h after plating. The ratio DNA:transfection agent (Neurofect, Genlantis, San Diego, CA) was 1:7. Neurons were left untreated at least for 48 h. The percent of neurons transfected was between 5 and 10%, as assessed with a GFP vector. In the day of the experiment, medium was replaced with Neurobasal + 25 mM KCl. Two hours later, IGF-I ($10^{-7}$ M) and/or $H_2O_2$ at doses of 50, 75, and 100 $\mu$M were added, whereas inhibitory drugs were given 45 min before treatments. We used $H_2O_2$ as an oxidant insult because it is an endogenously produced ROS that serves as a precursor to hydroxyl radicals and possesses signaling capacities (Finkel, 2003). Time schedule of the experiments is summarized in Figure 1A.

### *Cellular Fractionation*

Neural nuclear fractions were obtained from total lysates of granule neurons grown in 9-cm dishes, as described (Dignam *et al.*, 1983). Neural cytosolic fractions were obtained from neurons grown in six-well plates using as lysis buffer 4 mM $NaHCO_3$. The lysates were centrifuged at $1000 \times g$ for10 min to eliminate the nuclear fraction. Then, supernatants were centrifuged again at $22{,}000 \times g$ for 40 min to eliminate the membrane fraction. Cellular fractionation was assessed by assaying for nuclear proteins (Neu-N) in cytosolic extracts and for cytosolic proteins ($\beta$-actin) in nuclear extracts. Neu-N was detected in nuclear but not in cytosolic extracts, whereas $\beta$-actin was found only in cytosolic fractions.

### *Cell Assays*

Viability of neurons was assessed in different ways using 12-well plates. In a first assay, neurons were stained 6 h after respective treatments with propidium iodide (PI; Sigma, 2 $\mu$g/ml). PI-positive neurons were counted in a Leica CTR 6000 fluorescence microscope (Wetzlar, Germany). In another assay, neuronal cultures were transfected with a GFP-pCMV vector and the different constructs under evaluation in a 1:5 ratio. $GFP^+$ cells were scored before treatment to determine baseline survival (time 0) and at different times thereafter. In these two assays neurons were counted in three different fields per well at 40×. In a third type of assay the amount of lactate dehydrogenase (LDH) released from damaged neurons into the culture medium was used to quantify cell death. LDH levels were measured at various times with a commercial kit (Roche Diagnostics, Penzberg, Germany). In another type of assay, apoptotic cells were determined using a pan-specific fluorescent marker of activated caspases following the manufacturer's instructions (Promega, Madison, WI). Briefly, 6 h after the different treatments, 10 $\mu$M of CaspACE FITC-VAD-FMK was added to the cultures for 30 min. Then cells were washed three times with Neurobasal + 25 mM KCl, mounted, and photographed at 40×. Fluorescently labeled neurons were counted in three different fields per well. The number of stained cells was related to the total cell number determined with DAPI nuclear staining.

We also determined NADP and NADPH levels as an index of the redox status using a commercial colorimetric system (Biovision, Mountain View, CA). NADP/NADPH levels were measured in cell lysates 15 min after adding 50 $\mu$M $H_2O_2$ to the cultures (six-well dishes). Briefly, neurons were lysed and half of the lysate was used to measure total NADP/NADPH and the other half to measure NAPDH only. For the latter, NADP was decomposed by heating at 60°C for 30 min. The corresponding OD450-nm measurements were read in a NADPH standard curve to determine concentrations. The NADP/NAPDH ratio was calculated as (total NADP/NADPH-NADPH)/NADPH. All the above assays were done in triplicate dishes in at least three independent experiments.

In addition, generation of ROS was assessed with a superoxide anion assay kit from Sigma. The superoxide anion ($O_2^-$) is involved in redox signaling regulation,. The kit is based on the oxidation of luminol by $O_2^-$ and the resulting formation of chemiluminescence. Half a million neurons were added to luminometer tubes containing the reagents for luminol oxidation and different concentrations of $H_2O_2$ (0, 50, and 100 $\mu$M) in a final volume of 200 $\mu$l. Ten minutes later the chemiluminescence signal was determined. Assays were done in triplicate dishes.

### *Immunoassays*

Neuronal cultures were washed with PBS and fixed with 4% paraformaldehyde in 0.1 M phosphate buffer (PB) for 15 min. Cells were treated with 4% horse serum in 0.1 M PB for 1 h and washed three times for 10 min with 0.2% Triton and 0.3% BSA in 0.1 M PB. The cells were incubated with primary antibody overnight, rinsed with PBT, and incubated with secondary Alexa-tagged antibodies (Invitrogen) at 37°C for 1 h. Western blotting was performed as described (Garcia-Galloway *et al.*, 2003). Neurons were removed from the plates by washing once with ice-cold PBS and were lysed with PIK buffer (1% NP-40, 150 mM NaCl, 20 mM Tris, pH 7.4, 10% glycerol, 1 mM $CaCl_2$, 1 mM $MgCl_2$, 400 $\mu$M sodium vanadate, 0.2 mM PMSF, 1 $\mu$g/ml leupeptin, 1 $\mu$g/ml aprotinin, and 0.1% phosphatase inhibitor cocktails I and II of Sigma-Aldrich). To normalize for protein load, membranes were reblotted (ReBlot, Chemicon, Temecula, CA) and incubated with an appropriate control antibody (see *Results*). Levels of the protein under study were expressed relative to protein load in each lane as determined by appropriate control protein content. Different exposures of each blot were collected to ensure linearity and to match control levels for quantification. Densitometric analysis was performed using Analysis Image Program (Bio-Rad, Richmond, CA). A representative blot is shown from a total of at least three independent experiments (except when indicated). Immunoprecipitation was performed in

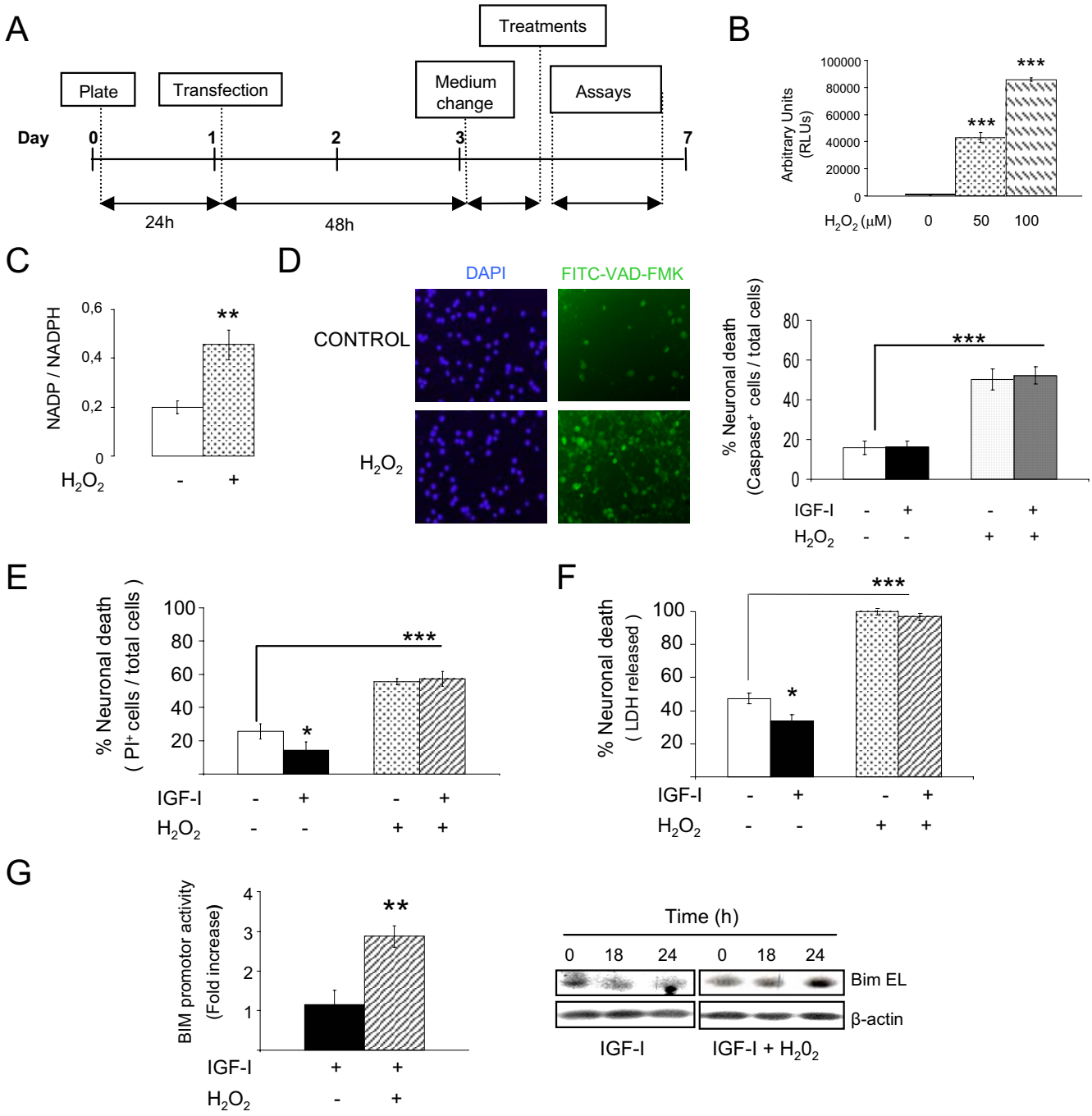


**Figure 1.** Neuronal death after exposure to hydrogen peroxide. (A) Time schedule of experiments. Cells were transfected 24 h after plating. Experiments were conducted in 3–7-d-old cultures, when neurons showed well developed neurites. (B) Addition of 50–100 $\mu$M $H_2O_2$ to the cultures generated reactive oxygen species (ROS; ***$p < 0.001$ vs. 0 dose) in a dose-dependent manner as determined by superoxide levels (RLUs arbitrary units), as well as a significant increase in the cellular NAD(P)/NAD(P)H ratio 15 min later (C), indicating a change in the redox status of the cell (**$p < 0.01$; $n = 3$). (D) Six hours after addition of 50 $\mu$M $H_2O_2$ to the cultures, many cells were apoptotic, as determined with a pan-active caspase fluorescent indicator (FITC-VAD-FMK) regardless of the presence of IGF-I. Histograms: quantitation of fluorescent-labeled cells ($n = 3$, $p < 0.001$ vs. controls). DAPI stain was used to mark all the cells in the cultures. (E) Neuronal death elicited by exposure to 50 $\mu$M $H_2O_2$ was also determined by percentage of dead neurons counting either propidium iodide-stained cells ($PI^+$) 6 h after insult, or (F) measuring LDH released to the medium 12 h after adding $H_2O_2$ (100% cell death corresponds to LDH levels in $H_2O_2$-treated cultures after 12 h). IGF-I (100 nM) protected neurons only in the absence of $H_2O_2$ (***$p < 0.001$ and *$p < 0.05$ vs. controls; $n = 3$). (G) Transcriptional activity of Bim EL is increased by $H_2O_2$ in IGF-I–treated neuronal cultures. Blots: protein levels of Bim EL were increased by $H_2O_2$ (10 $\mu$M) even though IGF-I was present. Actin levels are shown in lower blots. A representative experiment is shown (*$p < 0.05$ vs. IGF-I alone; $n = 3$ for both types of experiments).

cultured neurons lysed in PIK buffer and centrifuged at 22,000 × *g* for 20 min, and supernatants were incubated with primary antibody overnight. Protein A-agarose (Invitrogen) was added to the antigen–antibody mixture and incubated with gentle agitation overnight. The immunoprecipitate was washed

three times with the same lysis buffer, resuspended in 2.5× SDS loading buffer, electrophoresed, transferred to the nitrocellulose membrane, and analyzed by Western blot.

### *Luciferase Assays*

Neurons were transfected with a reporter construct bearing six canonical FOXO binding sites (6× DBE- luciferase) or a Bim promoter. Cells were cotransfected with different constructs as indicated in each experiment. Transfections were performed in triplicate dishes. Luciferase counts were normalized using TK-Renilla luciferase. At the given times, neurons were lysed in passive lysis buffer (PLB), and luciferase activity was analyzed using a luminometer and dual luciferase assay kit according to the manufacturer (Promega). Background luminescence was subtracted. Luciferase activity was expressed as fold of increase respect to control levels.

### *Statistical Analysis*

Data are expressed as mean ± SD. Differences among groups were analyzed by one-way ANOVA. Comparison between two groups was done with the *t* test. $p < 0.05$ was considered significant.

## RESULTS

### *Acute Oxidative Stress Triggers Neuronal Death Even in the Presence of the Neurotrophic factor IGF-I*

As reported by St-Pierre *et al.* (2006), addition of $H_2O_2$ to cultured cells generates an abrupt increase in ROS as measured by increased superoxide levels (Figure 1B) and, consequently, a change in the redox status of the cells (Figure 1C) as measured by relative levels of oxidized/reduced nicotinamide adenine dinucleotide phosphate [NAD(P)/NAD(P)H]. This abrupt increase in ROS levels elicited neuronal death, as reflected by robust increases in caspase activation in $H_2O_2$-treated cultures (Figure 1D).

Cell death induced by $H_2O_2$ was not blocked by the neurotrophic factor IGF-I in cerebellar neurons. Thus, addition of 50 $\mu$M $H_2O_2$ resulted in significant increases in cell death 6–12 h later, as determined by caspase activation (Figure 1D), PI nuclear staining (Figure 1E), or release to the medium of lactate dehydrogenase (Figure 1F), regardless of the presence of high levels (100 nM) of IGF-I. The effects of $H_2O_2$ were dose dependent (range of 10–50 $\mu$M) and maximal at 50 $\mu$M (100% of cells dead after 10–12 h). In accordance with a role of the transcription factor FOXO in $H_2O_2$-induced neuronal death (Lehtinen *et al.*, 2006), the promoter activity and protein levels of Bim EL, a proapoptotic protein downstream of FOXO, were increased after $H_2O_2$ (even at low doses of 10 $\mu$M) even in the presence of IGF-I (Figure 1G), whereas the antioxidant protein MnSOD, also downstream of FOXO, showed a nonsignificant trend to be increased (not shown).

We then explored the process whereby addition of $H_2O_2$ renders neurons insensitive to this growth factor. IGF-I exerts its neuroprotective actions through the PI3K/AKT pathway (Dudek *et al.*, 1997). Indeed, in the presence of PI3K inhibitors IGF-I does not rescue neurons from serum deprivation (not shown). In accordance with this, we found that addition of $H_2O_2$ rapidly resulted in decreased IGF-I–induced AKT phosphorylation (Figure 2A) in a dose-dependent manner (not shown) and reduced nuclear import of pAKT (Figure 2B). Levels of pAKT remained decreased for at least 4 h after $H_2O_2$, whereas total AKT levels were not modified (not shown).

Protective actions of IGF-I through PI3K/AKT involves inhibition of the activity of FOXO (Brunet *et al.*, 1999). Four hours after adding $H_2O_2$ (50 $\mu$M) to the cultures, FOXO3 (the major isoform in neurons) remained in the nuclear compartment even in the presence of IGF-I (Figure 2C, Supplementary Figure 1A), and its cytoplasmic export was inhibited: decreased levels of FOXO3 were found in the cytoplasm of IGF-I+$H_2O_2$-treated cells compared with IGF-I alone (Figure 2D). This was paralleled at later times by increased transcriptional activity of FOXO in the presence of $H_2O_2$+IGF-I, compared with IGF-I alone. Thus, neuronal cultures transfected with a FOXO-gene reporter system showed significantly greater FOXO activity 8 h after adding $H_2O_2$ even in the presence of IGF-I (Figure 2E). In addition, IGF-I–induced phosphorylation of FOXO3 in AKT-sensitive residues such as $Thr^{32}$ (not shown) or $Ser^{253}$ (Supplementary Figure 1B) was blocked by addition of $H_2O_2$.

That increased FOXO3 activity underlies neuronal death by $H_2O_2$ was confirmed by the observation that a DN FOXO3 significantly diminished the effect of $H_2O_2$, independently of the presence or absence of IGF-I. Neurons were cotransfected with GFP- and DN-FOXO3–expressing vectors. After 2 d, cultures received ±IGF-I (100 nM) ± $H_2O_2$ (50 $\mu$M) and the number of surviving neurons ($GFP^+$ cells) were counted 6 h later. As shown in Figure 2F, in the presence of DN-FOXO3 (2 $\mu$g), the number of surviving $GFP^+$ cells showed a ~20% decrease after treatment with $H_2O_2$, whereas in cultures transfected with the GFP vector alone (controls), $H_2O_2$ treatment elicited a significant ~50% decrease in cell numbers ($p < 0.001$ and $p < 0.01$ DN-FOXO3 vs. respective controls).

### *Oxidative Stress Inhibits IGF-I Signaling through p38α,β MAPK*

Because prolonged oxidative stress has been shown to interfere with IGF-I–induced IGF-I receptor (IGF-IR) auto-phosphorylation (Wu *et al.*, 2006), we analyzed whether treatment of primary neurons with bolus $H_2O_2$ also affected phosphorylation of the IGF-IR by IGF-I. However, treatment with $H_2O_2$ did not affect pTyr-IGF-IR levels after IGF-I stimulation (Supplementary Figure 1C). Even doses of 75 $\mu$M $H_2O_2$ had no effect (not shown). We next look for possible changes elicited by treatment with $H_2O_2$ downstream of the IGF-IR. After coaddition of 50 $\mu$M $H_2O_2$ and 100 nM IGF-I, decreased $Tyr^{612}$ phosphorylation of IRS-1 (Figure 3A, left blots) and enhanced phosphorylation at $Ser^{312}$ was observed (Figure 3A, right blots). At the same time, the interaction of IRS-1 with $p^{85}$PI3K was inhibited; i.e., less IRS-1 coimmunoprecipitated with $p^{85}$PI3K in the presence of $H_2O_2$ (Figure 3B). This correlated with increased association of IRS-1-14-3-3β, one of the 14-3-3 protein chaperones known to intervene in the differential Ser/Tyr-phosphorylation of IRS-1 (Supplementary Figure 1D).

Next, we searched for pathways involved in the attenuation of IGF-I signaling by $H_2O_2$. Involvement of the phosphatases PP1A and PP2A, that dephosphorylate IRS-1 and AKT, respectively, was ruled out using different doses of okadaic acid as a phosphatase inhibitor; i.e., the response to $H_2O_2$ remained unaltered (not shown). Using kinase-specific inhibitory drugs we also ruled out that JNK, diverse protein kinase C isoforms (α, βI, βII, γ, δ, ε, and ζ), cyclic-AMP-kinase, or mTor-kinase, all known to phosphorylate IRSs, mediated differential phosphorylation of IRS-1 after $H_2O_2$ (not shown). However, the p38α,β isoforms of the stress kinase MAPK appeared to be involved because SB239063, a p38α,β-specific inhibitor overruled the inhibitory effect of $H_2O_2$ on IRS-1 and FOXO3 phosphorylation (Figure 3, C and D). Accordingly, expression of DN-p38β MAPK, and to a less extent DN-p38α MAPK, by cerebellar neurons blocked the induction of FOXO activity after treatment with $H_2O_2$ (Figure 3E). Inhibition of p38 MAPK with SB239063 also blocked neuronal death by $H_2O_2$, as assessed by reduced number of PI-positive cells (Figure 3F) and reduced levels of

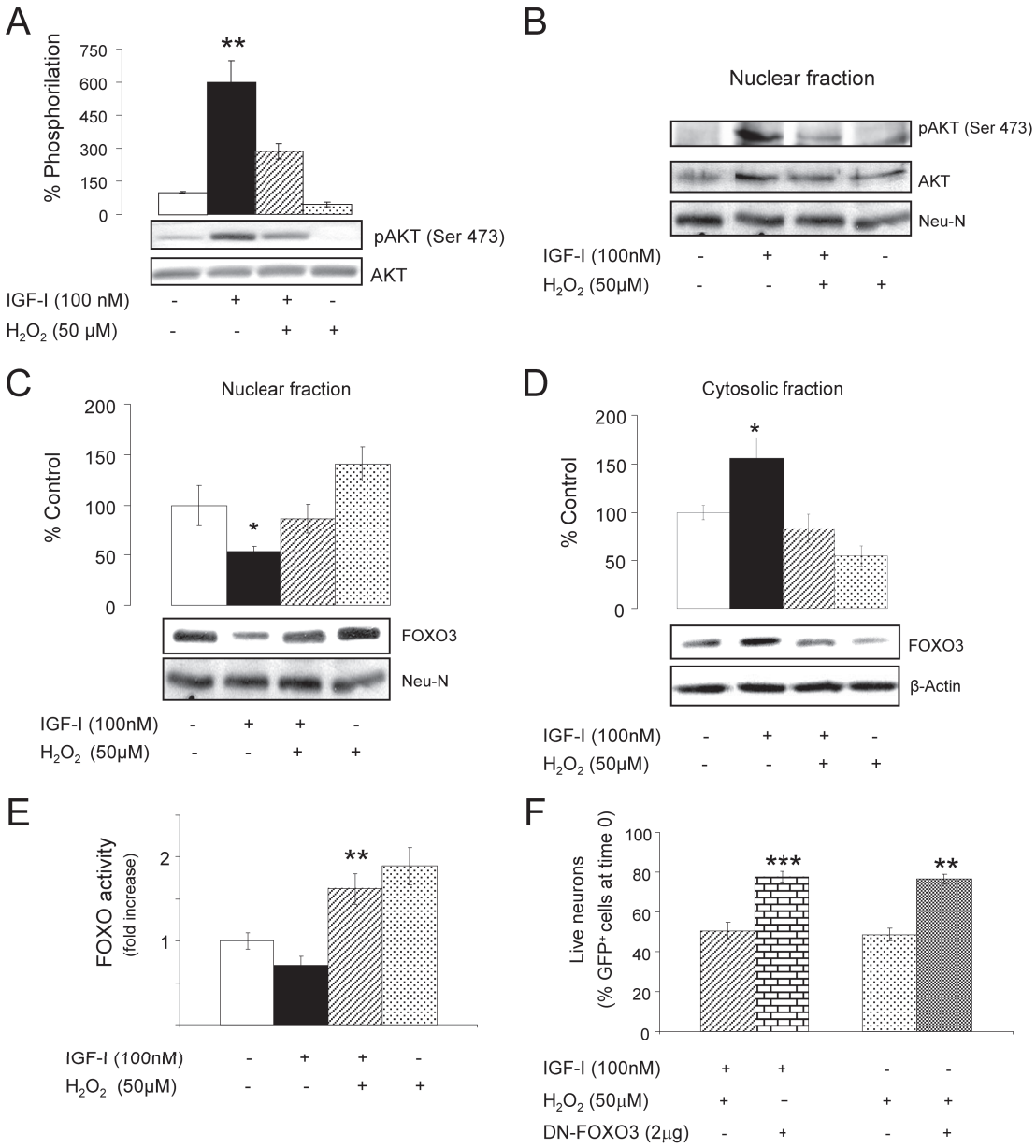


**Figure 2.** Modulation of AKT/FOXO by $H_2O_2$ in cerebellar neurons. (A) In the presence of $H_2O_2$, IGF-I–induced phosphoAKT (pAKT, 15 min after IGF-I) was significantly blocked. Levels of total AKT were measured as loading control. **$p < 0.01$ versus all other groups; n = 5. (B) Nuclear translocation of pAKT after IGF-I was blocked by $H_2O_2$. NeuN levels were determined as nuclear fraction control (n = 3). (C) In response to IGF-I levels of FOXO3 in the nucleus 4 h later were reduced, but this effect was blocked by $H_2O_2$. NeuN was used as a marker of the nuclear fraction; n = 3. (D) The opposite effect is observed with cytoplasmic levels of FOXO3, which were increased 4 h after IGF-I, and addition of $H_2O_2$ counteracted this effect. $\beta$-actin was measured as a marker of the cytosolic fraction (n = 4). (E) Transcriptional activity of FOXO was significantly attenuated by IGF-I after 8 h, but addition of $H_2O_2$ greatly enhanced it; n = 3. **$p < 0.01$ versus IGF-I–treated cells. (F) Neurons cotransfected with GFP and dominant negative (DN)-FOXO3 were protected against the deleterious effects of $H_2O_2$ compared with GFP-transfected neurons (controls), were a 40% drop in the number of $GFP^+$ cells was observed 6 h after treatment with $H_2O_2$, regardless of the presence or absence of IGF-1. ***$p < 0.001$, and **$p < 0.01$ versus controls (n = 3).

LDH in the culture medium (not shown) only when IGF-I was present.

### *Oxidative Stress Recruits a JNK2/FOXO3 Pathway in Neurons: Interactions with IGF-I Signaling*

Because treatment with $H_2O_2$ entirely blocked the prosurvival actions of IGF-I without producing a full reduction in IGF-I–induced AKT activity (measured as pAKT/AKT ratio), an additional "reinforcing" pathway to cell death could be postulated. We analyzed the potential involvement of JNK in $H_2O_2$-induced neuronal death because this stress kinase participates in the cellular actions of $H_2O_2$ (Kamata *et al.*, 2005) and activates FOXO4 (Essers *et al.*, 2004). The levels of phospho-JNK2 (the active form of this kinase) showed a slow but robust increase after adding $H_2O_2$ to IGF-I–treated neurons between 1 and 2 h (Figure 4, A and B), but not at earlier times (Supplementary Figure 1E), and returned to baseline levels 3 h later. Of note, IGF-I alone also

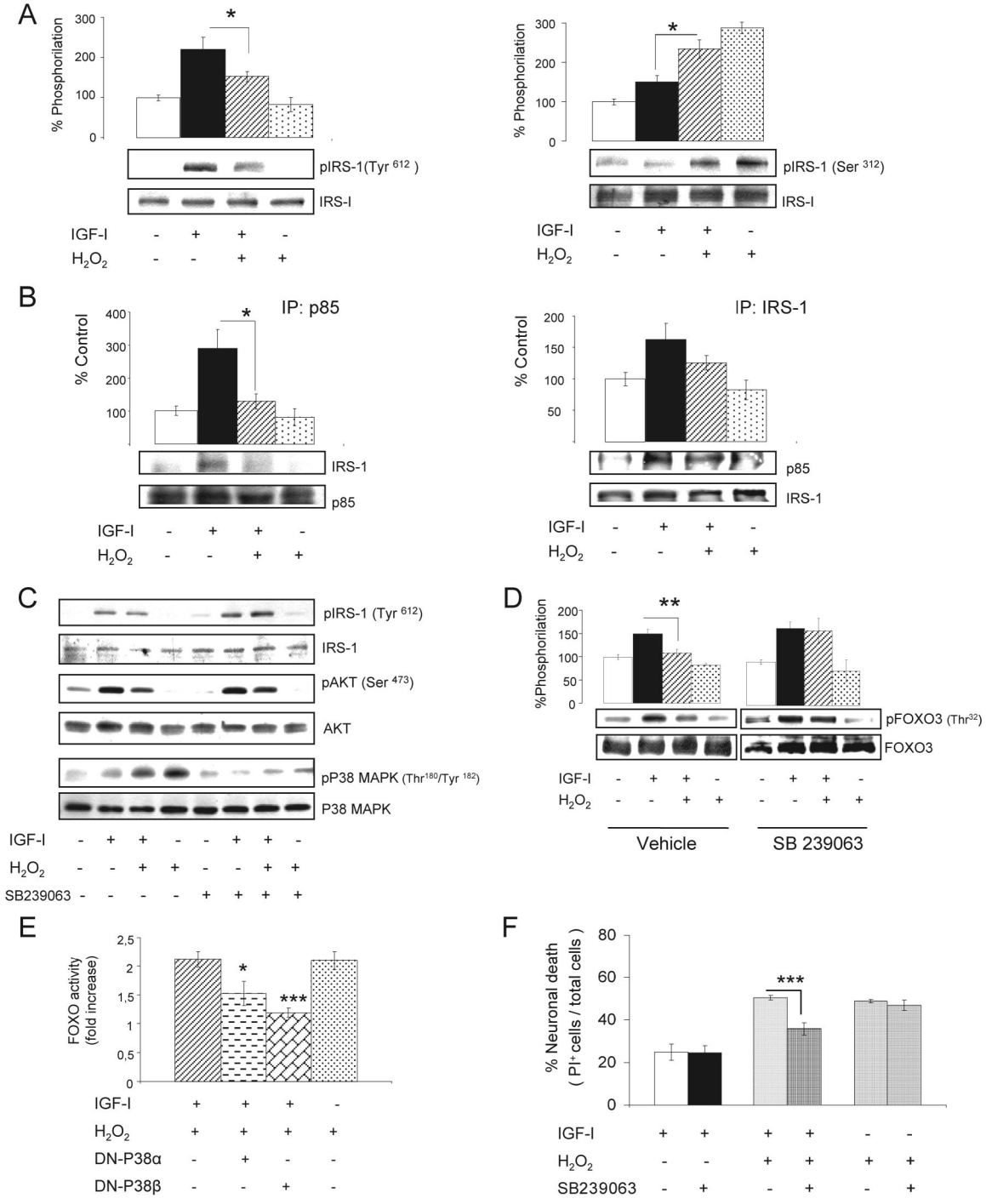


**Figure 3.** Reactive oxygen species inhibit IGF-I signaling in neurons. (A) Conjoint stimulation of cerebellar neurons with IGF-I and $H_2O_2$ (50 $\mu$M) resulted in reduction of Tyr-phosphorylation of IRS-1 15 min later, whereas Ser-phosphorylation of IRS-1 was enhanced 1 h later. Representative blots are shown. Histograms: densitometric quantification of blots. *$p < 0.05$; n = 3. (B) The presence of $H_2O_2$ in IGF-I–treated neuronal cultures also led to disrupted interaction of IRS-1 with PI3K, as less $p^{85}$PI3K coimmunoprecipitated with it. Association of IRS-1 to $p^{85}$PI3K 15 min after adding IGF-I was determined by reciprocal coimmunoprecipitation. Representative blots are shown. Histograms: densitometric quantification of blots. *$p < 0.05$ (n = 2 for each). (C) In the presence of 7.5 $\mu$M SB239063, a P38$\alpha$,$\beta$ MAPK inhibitor, $H_2O_2$ no longer induces the phosphorylation of this kinase, and Tyr-phosphorylation of IRS-1, and phosphoAKT (pAKT) in response to IGF-I is preserved (n = 3). Representative blots are shown. (D) In the presence of 7.5 $\mu$M SB239063, FOXO3 phosphorylation at the AKT-sensitive $Thr^{32}$ residue by IGF-I is preserved. Representative blots are shown. Histograms: densitometry of blots. **$p < 0.01$; n = 3. (E) Neuronal cultures transfected with a DN-p38$\beta$ MAPK before exposure to IGF-I+ $H_2O_2$ showed markedly reduced FOXO transcriptional activity in response to $H_2O_2$. Cultures transfected with a DN-p38$\alpha$ MAPK showed also, albeit smaller, a reduction in FOXO activity. *$p < 0.05$ and ***$p < 0.001$ versus controls; n = 3. (F) The P38$\alpha$,$\beta$ MAPK inhibitor SB239063 blocked $H_2O_2$-induced cell death in IGF-I–treated cultures, as assessed by the number of $PI^+$ cells 6 h later. *$p < 0.05$ versus controls; n = 3 for each assay.

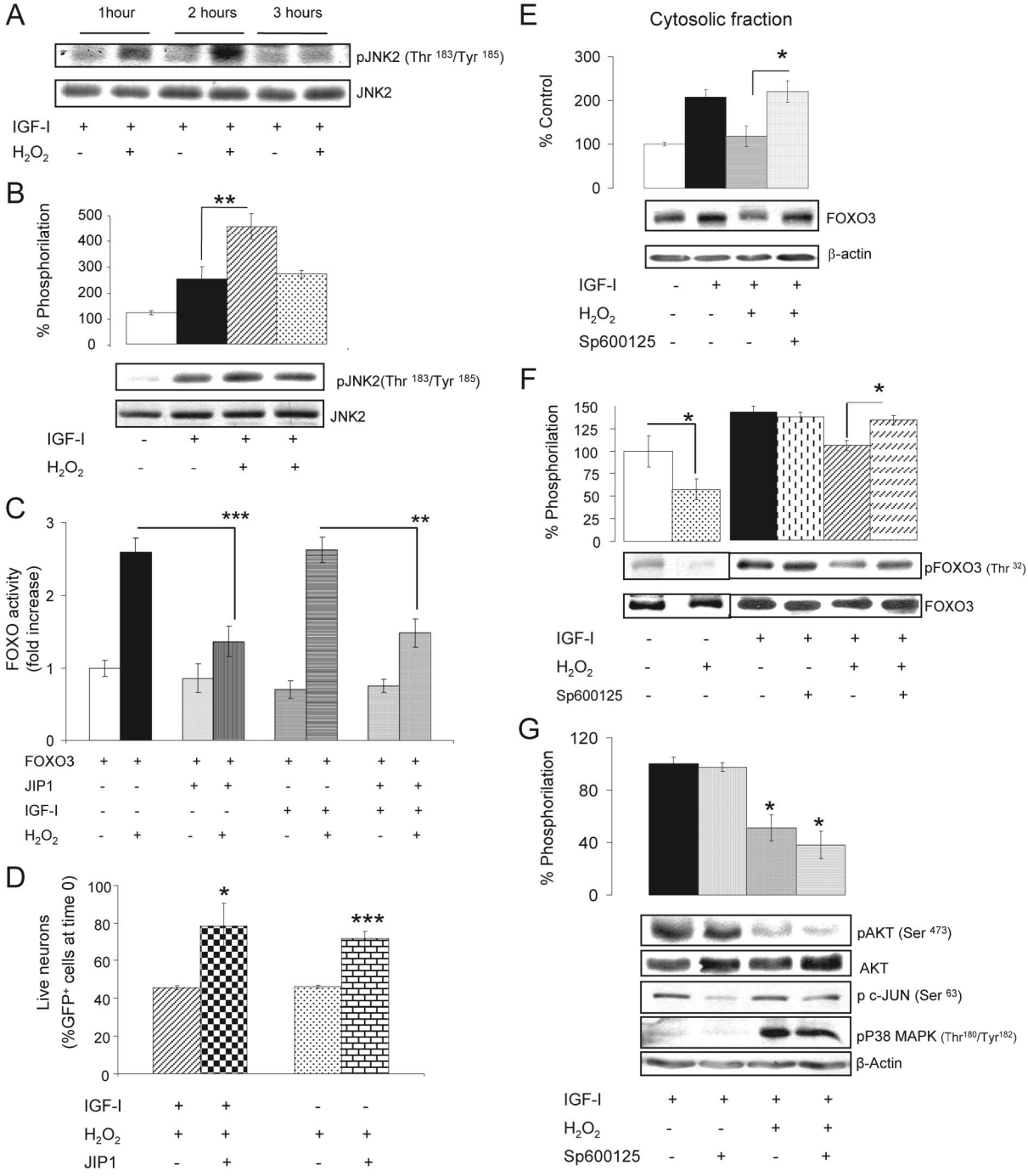


**Figure 4.** Role of JNK in $H_2O_2$-induced neuronal death. (A) Addition of $H_2O_2$ to IGF-I–treated cerebellar neurons produced a delayed increase in JNK2 activity as determined by enhanced levels of phospho-JNK2 (pJNK2) between 1 and 2 h later; n = 3. (B) Densitometric quantification of the increase in pJNK2 at 2 h. Representative blot is shown below; n = 4. (C) Transfection of the JNK inhibitor JIP-1 to neurons was sufficient to reduce activation of FOXO by $H_2O_2$ regardless of IGF-I. Neuronal cultures were cotransfected with WTFOXO3- and JIP-1–expressing vectors and FOXO activity was measured in luciferase gene reporter assays. $^{**}p < 0.01$ and $^{***}p < 0.001$; n = 4. (D) Neuronal death is substantially abrogated when JIP-1 is expressed in ±IGF-I–treated neurons before addition of $H_2O_2$. $^{*}p < 0.05$, and $^{***}p < 0.001$ versus respective JIP-1–expressing cultures; n = 3. Cell death was assessed as number of $GFP^+$ cells 6 h after adding $H_2O_2$ and expressed as percentage of $GFP^+$ cells at time 0. (E) After addition of Sp600125 (20 $\mu$M), an inhibitor of JNKs, translocation of FOXO3 from the nucleus to the cytoplasm by IGF-I is preserved in the presence of $H_2O_2$ in the cultures. $\beta$-actin levels were measured as control of the cytoplasmic fraction. Histograms: densitometric quantification of blots. $^{*}p < 0.05$; n = 3. (F) Sp600125 restored FOXO3 phosphorylation by IGF-I at the AKT-sensitive $Thr^{32}$ residue, even in the presence of $H_2O_2$. Histograms: quantification of $pThr^{32}FOXO3$ corrected for total FOXO3. ($^{*}p < 0.05$; n = 5). Control experiments in the absence of IGF-I are shown in a separate representative blot in the left ($^{*}p < 0.05$; n = 3). (G) Levels of pAKT remained reduced after treatment of IGF-I–treated cultures with $H_2O_2$ when Sp600125 was present. This correlated with intact activation of p38MAPK by $H_2O_2$. Inhibition of JNK by Sp600125 was corroborated by inhibition of phosphorylation of c-Jun (a downstream target of JNK). Histograms: quantification of pAkt corrected for total Akt ($^{*}p < 0.05$ vs. respective control; n = 4). Representative blots are shown in all panels.

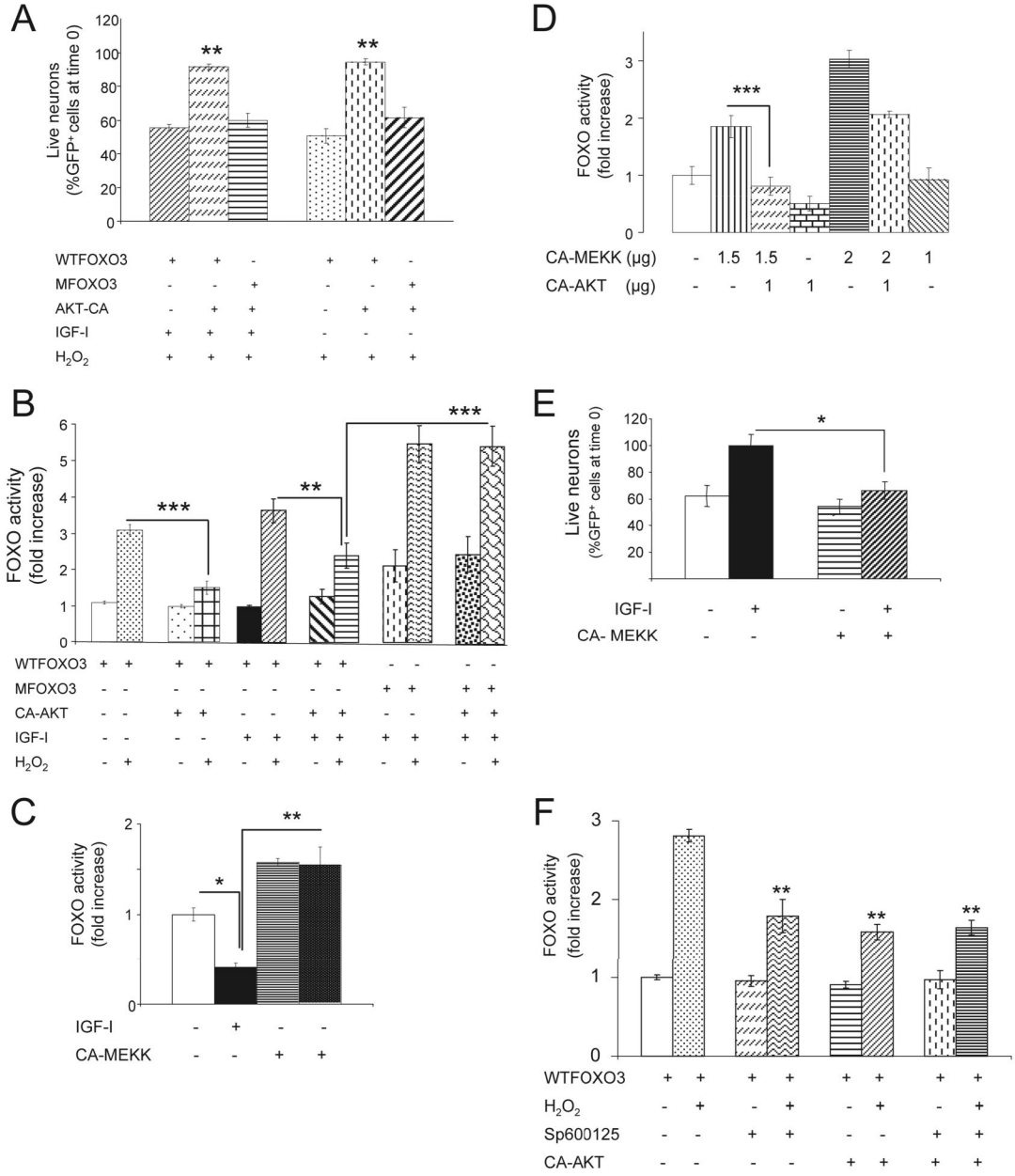


**Figure 5.** An interplay of AKT and JNK onto FOXO activity. (A) Expression of a constitutively active (CA) form of AKT resulted in abrogation of cell death by $H_2O_2$ even in the absence of IGF-I (right-hand bars). Cotransfection of GFP, WTFOXO3 and CA-AKT expressing vectors inhibits neuronal death after $H_2O_2$ compared with cultures cotransfected with control vector, GFP- and WTFOXO3-expressing vectors. Live neurons are expressed as percentage of $GFP^+$ cells at time 0. $^{**}p < 0.01$, n = 2. (B) Transcriptional activity of FOXO is robustly modulated by AKT. Cotransfection of CA-AKT with WTFOXO3 results in markedly reduced FOXO activity after $H_2O_2$ regardless of IGF-I. In contrast, cotransfection of CA-AKT with an AKT-insensitive mutant (M) FOXO3 results in preservation of enhanced FOXO activity after $H_2O_2$. $^{**}p < 0.01$ and $^{***}p < 0.001$ versus indicated groups; n = 4. (C) Transcriptional activity of FOXO is enhanced by MEKK, which in turn counteracts the inhibitory action of IGF-I. $^{*}p < 0.05$ and $^{**}p < 0.01$ versus indicated groups; n = 3. (D) Antagonistic regulation of FOXO activity by MEKK and AKT, respectively. AKT was able to counteract the stimulatory effect of MEKK onto FOXO in a dose-dependent way. Neuronal cultures were cotransfected with various amounts of the respective vectors, and FOXO activity was determined with a luciferase gene-reporter system. $^{***}p < 0.001$ versus CA-AKT–cotransfected cultures; n = 3. (E) Expression of MEKK in neuronal cultures resulted in increased cell death as determined by the number of $GFP^+$ cells. Cultures were cotransfected with GFP- and CA-MEKK– or GFP-expressing vectors only (controls) with or without IGF-I, and the number of cells was scored 24 h later. $^{*}p < 0.05$ versus IGF-I–treated cultures; n = 3. (F) Partial abrogation of $H_2O_2$-induced FOXO activity by expression of CA-AKT (1 $\mu$g) was not modified by addition of the JNK inhibitor Sp600125. Note that inhibition of FOXO activity was similar by either inhibition of JNK or stimulation of AKT ($p < 0.01$ vs. $H_2O_2$-treated cultures (dotted bar); n = 3).

elicited a delayed, albeit smaller increase in this kinase (see Figure 4B). Levels of pJNK1 isoform were also elevated, but in a less consistent manner (not shown). Because addition of $H_2O_2$ elicited stimulation of p38 MAPK within minutes, whereas JNK2 was stimulated at later times, we determined whether JNK activation was downstream of p38 MAPK.

However, inhibition of p38 MAPK with SB239063 resulted in enhanced basal levels of pJNK2 and did not interfere with $H_2O_2$-induced stimulation (not shown), indicating that activation of JNK2 after $H_2O_2$ is not due to prior activation of p38.

That JNK was involved in neuronal death after $H_2O_2$ in IGF-I–treated cells was confirmed by the following experiments. In cultures cotransfected with JIP1 to inhibit JNKs (Heo *et al.*, 2004), and with wild-type (WT) FOXO3, addition of $H_2O_2$ to ±IGF-I–treated cells resulted in a markedly lower increase in FOXO activity (Figure 4C; $p < 0.01$), suggesting that JNK activity (which is blocked by JIP1; not shown) is necessary for the full effect of $H_2O_2$ on FOXO activation. Importantly, decreased FOXO activity in the presence of JIP1 correlated with significantly less neuronal death after $H_2O_2$, even in the absence of IGF-I (Figure 4D). Thus, in IGF-I–treated cultures cotransfected with a GFP- and a JIP1-expressing vector only a ~20% reduction in $GFP^+$ cells was seen after $H_2O_2$ as compared with a ~60% reduction in cultures transfected with a GFP control vector ($p < 0.05$).

Additional experiments provided further evidence that JNK is involved in the deleterious actions of $H_2O_2$ on neurons. For instance, inhibition of JNKs with SP600125 (20 $\mu$M) blocked the inhibitory action of $H_2O_2$ on IGF-I–induced cytoplasmic accumulation of FOXO3 (Figure 4E) and pFOXO3 (not shown). Administration of SP600125 to the cultures also restored IGF-I–induced phosphorylation of FOXO3 at the AKT-sensitive $Thr^{32}$ (Figure 4F) and $Ser^{253}$ (not shown) residues in the presence of $H_2O_2$. Importantly, pAKT levels remained decreased after adding $H_2O_2$ even in the presence of the JNK inhibitor (Figure 4G). This correlated with preserved phosphorylation of p38 MAPK after adding $H_2O_2$ (Figure 4G). The latter observation confirms that stimulation of p38 and JNK by treatment with $H_2O_2$ occurs through independent pathways.

To test whether competition between AKT and JNK over FOXO (Kops *et al.*, 2002) underlies the antagonism between IGF-I and $H_2O_2$ in neurons, we modulated the activity of either AKT or JNK. Neuronal expression of a constitutively active (CA) AKT blocked $H_2O_2$-induced neuronal death. The number of surviving $GFP^+$ cells were only slightly decreased (~10% of time 0) 6 h after addition of $H_2O_2$ when cultures were cotransfected with CA-AKT and WT FOXO3, even in the absence of IGF-I, but still significantly decreased in control cultures cotransfected with empty vector and WT FOXO3 ($p < 0.01$ vs. all other groups; Figure 5A). Measurement of FOXO activity confirmed this observation because in the presence of CA-AKT, FOXO was significantly less activated by treatment with $H_2O_2$ ($p < 0.001$ vs. control vector–transfected neurons; Figure 5B). In agreement, the inhibitory action of $H_2O_2$ on IGF-I–induced phosphorylation of FOXO3 on $Thr^{32}$ residues was also blocked by CA-AKT (not shown). We also confirmed that abrogation of the deleterious effects of $H_2O_2$ on neurons depends on inhibition of FOXO by AKT. In neurons expressing a mutant form of FOXO3 insensitive to AKT (MFOXO3, where AKT-sensitive residues have been mutated) the number of surviving $GFP^+$ cells was significantly decreased after $H_2O_2$ ($p < 0.01$ vs. WT FOXO-transfected cells, Figure 5A). Indeed, in the presence of MFOXO3, CA-AKT was unable to impede activation of FOXO after treatment with $H_2O_2$ (Figure 5B).

Conversely, activation of JNK in the cultures through expression of a constitutively active (CA) form of MEKK, a stimulatory JNK kinase (not shown), blocked the inhibitory action of IGF-I on FOXO activity, mimicking the action of $H_2O_2$ (Figure 5C). The effect of MEKK on FOXO depended on the level of AKT activity. Thus, FOXO activity was dose-dependently and antagonistically regulated by CA-MEKK and CA-AKT, respectively (Figure 5D). Higher expression of CA-MEKK resulted in higher FOXO activity and conversely, higher CA-AKT induced lower FOXO activity. As expected based on the ability to mimic the action of $H_2O_2$, expression of CA-MEKK in IGF-I–treated cultures resulted in increased neuronal death measured 24 h later (Figure 5E). An additional experiment indicated that blockade of either inhibition of AKT or stimulation of JNK in response to $H_2O_2$ is sufficient to abrogate the activation of FOXO. Thus, partial abrogation of FOXO activity in $H_2O_2$-exposed cultures transfected with WTFOXO by coexpression of CA-AKT was not augmented by addition of the JNK inhibitor SP600125, which alone produced an equivalent reduction of FOXO activity (Figure 5F). This data confirm that an interplay between AKT and JNK dictate the FOXO response to $H_2O_2$.

We next performed several experiments to start analyzing possible mechanisms underlying activation of FOXO after addition of $H_2O_2$. Because JNK is a Ser-kinase, we used the mutant form of MFOXO3, where all three AKT-sensitive residues are mutated, to determine whether $H_2O_2$ was able to induce the phosphorylation of MFOXO3 at Ser residues other than those modulated by AKT. We found that total Ser-phosphorylation was dose-dependently induced after $H_2O_2$ in HA.MFOXO3-transfected neurons (Figure 6A). As expected, this effect was dependent on JNK because cotransfection of the neuronal cultures with JIP1 (not shown) or addition of the JNK inhibitor Sp600125 abrogated it (Figure 6B). In preliminary experiments we also observed that addition of $H_2O_2$ induced uncoupling of FOXO with 14-3-3 protein chaperones, as already documented in detail by others (Lehtinen *et al.*, 2006), whereas IGF-I promoted their

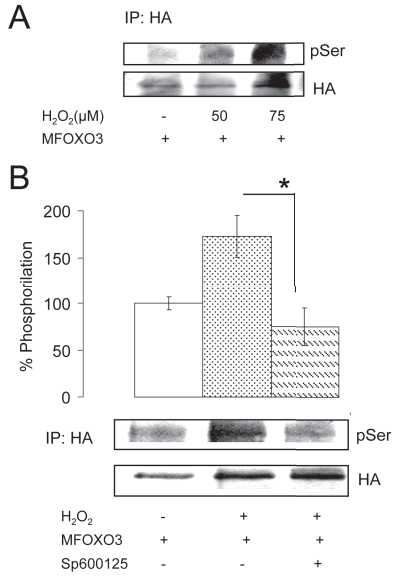


**Figure 6.** Activation of FOXO3 by $H_2O_2$ through JNK involves Ser phosphorylation. (A) Cerebellar neurons transfected with an HA-tagged MFOXO3 (where AKT-sensitive residues have been mutated) show dose-dependent increases in Ser-phosphorylation (pSer) levels after addition of $H_2O_2$. Cell extracts were immunoprecipitated with anti-HA antibodies 4 h after exposure to $H_2O_2$, and levels of pSer in immunoprecipitates were determined; n = 3. (B) Addition of the JNK inhibitor Sp600125 to HA.MFOXO3–transfected neuronal cultures abrogated PSer by 75 $\mu$M $H_2O_2$ measured 4 h later. Representative blots are shown; n = 3. Coexpression of the JNK inhibitor JIP-1 instead of adding the JNK inhibitor produced an identical effect (not shown). *$p < 0.05$.

association (not shown). We finally explored whether AKT influence JNK (Park *et al.*, 2002) and found that inhibition of AKT with LY294002 did not alter stimulation of JNK2 after $H_2O_2$ (not shown).

## DISCUSSION

The mechanisms underlying oxidative cell death constitute a very important aspect of current research into the causes of neurodegenerative diseases (Beal, 1995). Under physiological conditions tightly controlled levels of endogenous ROS are also utilized by the cell to modulate redox-sensitive processes (Droge, 2002). In theory, imbalanced ROS production may lead to cell death in part also through disturbances in these redox-sensitive pathways. However, the mechanisms involved in the transition from normal ROS physiology to oxidant-mediated cell death are not fully described. In the present study we focused on the effects of ROS on IGF-I signaling and its role in neuronal death. This trophic pathway is probably affected by excess ROS because under normal physiology several of its components are redox-sensitive. Thus, redox status determines the activity of several phosphatases that negatively impinge on IGF-I signaling (by modulating PI3K, IRS-1, or the tyrosine kinase activity of the receptor) by reversibly modulating SH-bonds in specific cysteine residues. IGF-I and insulin signaling also include generation of ROS through NADP as an active signaling component. In the presence of high ROS levels and oxidized NADP both routes will be likely affected. An important reason to focus on IGF-I signaling is because this pathway is an important determinant of neuronal survival (Mahadev *et al.*, 2001; Lee *et al.*, 2002; Trejo *et al.*, 2004).

Our results indicate that neuronal death after an abrupt increase in oxidative stress takes places through a two-arm mechanism that involves inhibition of the protective actions of IGF-I: 1) blockade through p38 MAPK of the inhibition of the transcription factor FOXO by AKT, a prosurvival kinase modulated by trophic factors such as IGF-I, and 2) subsequent activation of FOXO by JNK. These two pathways are independently activated in response to ROS; JNK is activated even if p38 is inhibited, whereas p38 remains active even when JNK is blocked. However, the two of them need to be active to induce cell death by ROS. In the first arm of this pathway, excess ROS (mimicked by addition of $H_2O_2$ to the cultures) uncoupled IRS-1/$p^{85}$PI3K interactions by Ser phosphorylation of IRS-1 through the stress kinase p38 MAPK, resulting in partial inhibition of AKT. This mechanism appears essential to allow activation of FOXO by JNK; the observed competitive deactivation/activation interplay between AKT and JNK onto FOXO would otherwise impede activation of FOXO. Whether JNK directly phosphorylates FOXO3, as shown with FOXO4 (Essers *et al.*, 2004) or the

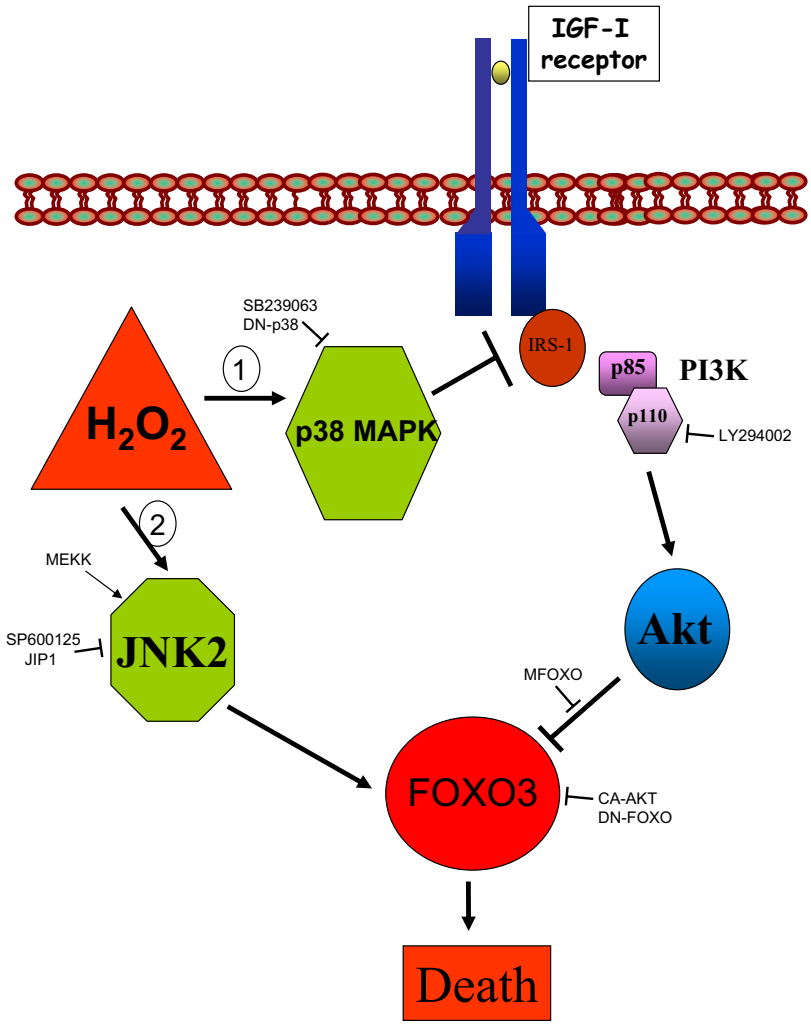


**Figure 7.** Inhibition of IGF-I signaling is involved in neuronal death after $H_2O_2$. A competitive interplay between AKT and JNK in regulating FOXO3 activity dictates the neuronal response to an abrupt rise in ROS elicited by $H_2O_2$. Cytotoxic levels of $H_2O_2$ sequentially activate two independent pathways. A rapid route (1) includes activation of p38 MAPK to inhibit IGF-I signaling by interfering IGF-I receptor/IRS-1 interactions through phosphorylation of serine residues in IRS-1. This leads to abrogation of AKT inhibition of FOXO. A delayed route (2) recruits JNK2 to activate FOXO. Activation of the p38 MAPK pathway is essential because JNK is unable to activate FOXO if AKT is active. Conversely, once JNK activates FOXO, it becomes refractory to inactivation by AKT. The different inhibitory drugs and stimulatory and inhibitory DNA constructs used in this study are indicated.

process involves other kinases (Lehtinen *et al.*, 2006) would require further work. At any rate, phosphorylation of FOXO3 at serine residues depended on JNK activity and involved residues different from those phosphorylated by AKT. Phosphorylation of these residues by this JNK pathway could explain the inability of IGF-I/AKT to inhibit FOXO once it is activated by JNK. In turn, the predominant nuclear distribution of JNK2 in cerebellar neurons (Coffey *et al.*, 2002) may explain the need to abrogate the inhibitory action of AKT on FOXO3 to allow its subsequent activation by JNK. Thus, phosphorylation of FOXO3 by AKT results in its translocation to the cytoplasm; if this process is inhibited, FOXO3 would remain available in the nucleus to be activated by JNK2.

The transcription factor family FOXO has been involved in cell death processes and in the response to oxidative stress (van der Horst and Burgering, 2007). FOXO3 seems to carry out both activities simultaneously (Brunet *et al.*, 2004). However, it seems that after an abrupt rise in ROS the proapoptotic activity of FOXO3 predominated in neurons: BimEL activity increased, whereas inactivation of FOXO3 resulted in enhanced neuronal survival. These results agree and extend previous observations of ROS-mediated inhibition of IGF-I/insulin signaling (Zhong and Lee, 2007) and of the important role of FOXO activation after exposure to ROS in neuronal death (Lehtinen *et al.*, 2006). They also shed light into an important aspect of ROS-mediated neurodegeneration, namely, whether the pathological mechanisms set in motion by chronic oxidative stress (as in progressive neurodegenerative diseases) have the same etiopathogenic significance as those produced by oxidant bursts (as in ischemia, epilepsy, or trauma). Although the former appear to inhibit IGF-I/insulin signaling through unspecific protein oxidation (Wu *et al.*, 2006), the latter specifically target these pathways by Ser phosphorylation of IRS (Houstis *et al.*, 2006). Therefore, chronic oxidative stress appears as a progression factor in protracted neurodegeneration, whereas oxidant bursts may underlie rapid neuronal loss.

We speculate that this level-dependent role of oxidative stress is related to the activity status of AKT in neurons. Thus, relatively low levels of ROS during chronic oxidative stress will not inactivate IGF-I signaling, and therefore AKT will remain active so FOXO will not be activated by JNK. Our results show that the ability of $H_2O_2$ to activate FOXO in the presence of IGF-I depends on the amount of active AKT. Indeed, neurons become specially vulnerable to acute oxidative stress when the levels of active AKT are low (Taylor *et al.*, 2005). The opposite is also true, that is, the ability of AKT to inactivate FOXO depends on the levels of active JNK. A similar competitive interplay was described for the apoptotic protein BAD, where BAD phosphorylation by JNK inhibited BAD inactivation by AKT (Donovan *et al.*, 2002). Therefore, a balance between AKT activity (determined by the level of trophic input) and JNK activity (determined by the level of ROS input) within the neuron will determine the response to ROS. Because both pathways are redox-sensitive (Lee *et al.*, 2002; Leslie, 2006), we can conclude that ROS levels dictate neuronal health by regulating the status of FOXO activity through this competitive regulatory process. Therefore, whether neurons survive or not during the neurodegenerative process will be determined by the balance between levels of ROS, that enhance JNK activity and depress AKT activity, and levels of the different trophic factors known to stimulate AKT, such as IGF-I. A practical consequence of our observations is that free radical scavengers will enhance the neuroprotective activity of IGF-I and other growth factors and may be of potential utility as therapeutic adjuvants of neuroprotective drugs.

All the pathways described herein have already been shown to participate in cell death by oxidative stress under different circumstances. However, integration of all of them into a single process of neuronal death was not documented before (see Figure 7). Thus, activation of ser-kinases by $H_2O_2$ has been reported (Migliaccio *et al.*, 1999), and in particular of the stress kinases JNK and p38MAPK (Clerk *et al.*, 1998), with many different routes involved (Finkel, 2003). In addition, a higher activation of JNK2 versus JNK1 by oxidative stress was also shown (Coffey *et al.*, 2002). Similarly, antagonistic effects of JNK on IGF-I/insulin signaling have also been reported (Essers *et al.*, 2004). Although FOXO was already shown to mediate cell death by hydrogen peroxide in cerebellar neurons, whether JNK was involved in this effect remained undefined (Lehtinen *et al.*, 2006) and the significance of p38 MAPK was also undetermined. We now connect ROS interference of IGF-I/insulin signaling with ROS-mediated neuronal death via FOXO, showing that the first process seems to be necessary for the progress of the second. This connection integrates two previously unrelated pathways into a unique comprehensive pathway.

Because interference with IGF-I signaling on neurons is involved not only in cell death by oxidative stress but also in inflammatory and excitotoxic neuronal loss (Venters *et al.*, 1999; Garcia-Galloway *et al.*, 2003), diminished IGF-I signaling may be considered a common determinant in cell death associated to neurodegeneration in where these pathological processes are participating (Trejo *et al.*, 2004). IGF-I sensitizers may therefore be of benefit in a wide array of neurodegenerative diseases. Specifically, AKT mimetics coupled to p38 and JNK inhibitors may constitute an amenable therapeutic cocktail in neurodegenerative diseases involving excess ROS.

In summary, high levels of oxidative stress triggers cell death in neurons by a compounded process involving sequential activation of two stress kinases (p38 and JNK) as well as inhibition of the neuroprotective IGF-I/AKT pathway. Importantly, both events are required to activate the transcription factor FOXO that turns on an apoptotic cascade.

## ACKNOWLEDGMENTS

We acknowledge the generosity of the numerous colleagues that provided the different constructs. We are thankful to M. Oliva and L Guinea for technical support. This work was funded by Grants SAF2001-1722 and 2004-0446 to I.T.A. and a contract from CIBERNED to D.D.

## REFERENCES

Aguirre, V., Werner, E. D., Giraud, J., Lee, Y. H., Shoelson, S. E., and White, M. F. (2002). Phosphorylation of Ser307 in insulin receptor substrate-1 blocks interactions with the insulin receptor and inhibits insulin action. J. Biol. Chem. *277*, 1531–1537.

Beal, M. F. (1995). Aging, energy, and oxidative stress in neurodegenerative diseases. Ann. Neurol. *38*, 357–366.

Behl, C., Davis, J. B., Lesley, R., and Schubert, D. (1994). Hydrogen peroxide mediates amyloid beta protein toxicity. Cell *77*, 817–827.

Biggs, W. H., III, Meisenhelder, J., Hunter, T., Cavenee, W. K., and Arden, K. C. (1999). Protein kinase B/Akt-mediated phosphorylation promotes nuclear exclusion of the winged helix transcription factor FKHR1. Proc. Natl. Acad. Sci. USA *96*, 7421–7426.

Brunet, A., Bonni, A., Zigmond, M. J., Lin, M. Z., Juo, P., Hu, L. S., Anderson, M. J., Arden, K. C., Blenis, J., and Greenberg, M. E. (1999). Akt promotes cell survival by phosphorylating and inhibiting a Forkhead transcription factor. Cell *96*, 857–868.

Brunet, A. *et al.* (2004). Stress-dependent regulation of FOXO transcription factors by the SIRT1 deacetylase. Science *303*, 2011–2015.

Clerk, A., Fuller, S. J., Michael, A., and Sugden, P. H. (1998). Stimulation of "stress-regulated" mitogen-activated protein kinases (stress-activated protein

kinases/c-Jun N-terminal kinases and p38-mitogen-activated protein kinases) in perfused rat hearts by oxidative and other stresses. J. Biol. Chem. *273*, 7228–7234.

Coffey, E. T., Smiciene, G., Hongisto, V., Cao, J., Brecht, S., Herdegen, T., and Courtney, M. J. (2002). c-Jun N-terminal protein kinase (JNK) 2/3 is specifically activated by stress, mediating c-Jun activation, in the presence of constitutive JNK1 activity in cerebellar neurons. J. Neurosci. *22*, 4335–4345.

De Fea, K. and Roth, R. A. (1997). Protein kinase C modulation of insulin receptor substrate-1 tyrosine phosphorylation requires serine 612. Biochemistry *36*, 12939–12947.

Dignam, J. D., Lebovitz, R. M., and Roeder, R. G. (1983). Accurate transcription initiation by RNA polymerase II in a soluble extract from isolated mammalian nuclei. Nucleic Acids Res. *11*, 1475–1489.

Donovan, N., Becker, E. B., Konishi, Y., and Bonni A. (2002). JNK phosphorylation and activation of BAD couples the stress-activated signaling pathway to the cell death machinery. J. Biol. Chem. *277*, 40944–40949.

Dringen, R., Pawlowski, P. G., and Hirrlinger, J. (2005). Peroxide detoxification by brain cells. J. Neurosci. Res. *79*, 157–165.

Droge, W. (2003). Oxidative stress and aging. Adv. Exp. Med. Biol. *543*, 191–200.

Droge, W. (2002). Free radicals in the physiological control of cell function. Physiol. Rev. *82*, 47–95.

Dudek, H., Datta, S. R., Franke, T. F., Birnbaum, M. J., Yao, R., Cooper, G. M., Segal, R. A., Kaplan, D. R., and Greenberg, M. E. (1997). Regulation of neuronal survival by the serine-threonine protein kinase Akt. Science *275*, 661–665.

Essers, M. A., Weijzen, S., de Vries-Smits, A. M., Saarloos, I., de Ruiter, N. D., Bos, J. L., and Burgering, B. M. (2004). FOXO transcription factor activation by oxidative stress mediated by the small GTPase Ral and JNK. EMBO J. *23*, 4802–4812.

Fernandez, A. M., Gonzalez de la Vega, A. G., Planas, B., and Torres-Aleman, I. (1999). Neuroprotective actions of peripherally administered insulin-like growth factor I in the injured olivo-cerebellar pathway. Eur. J. Neurosci. *11*, 2019–2030.

Finkel, T. (2003). Oxidant signals and oxidative stress. Curr. Opin. Cell Biol. *15*, 247–254.

Garcia-Galloway, E., Arango, C., Pons, S., and Torres-Aleman, I. (2003). Glutamate excitotoxicity attenuates insulin-like growth factor-i prosurvival signaling. Mol. Cell Neurosci. *24*, 1027–1037.

Gilley, J., Coffer, P. J., and Ham, J. (2003). FOXO transcription factors directly activate bim gene expression and promote apoptosis in sympathetic neurons. J. Cell Biol. *162*, 613–622.

Hansen, L. L., Ikeda, Y., Olsen, G. S., Busch, A. K., and Mosthaf, L. (1999). Insulin signaling is inhibited by micromolar concentrations of H(2)O(2). Evidence for a role of H(2)O(2) in tumor necrosis factor alpha-mediated insulin resistance. J. Biol. Chem. *274*, 25078–25084.

Heo, Y. S. *et al.* (2004). Structural basis for the selective inhibition of JNK1 by the scaffolding protein JIP1 and SP600125. EMBO J. *23*, 2185–2195.

Houstis, N., Rosen, E. D., and Lander, E. S. (2006). Reactive oxygen species have a causal role in multiple forms of insulin resistance. Nature *440*, 944–948.

Kamata, H., Honda, S., Maeda, S., Chang, L., Hirata, H., and Karin, M. (2005). Reactive oxygen species promote TNFalpha-induced death and sustained JNK activation by inhibiting MAP kinase phosphatases. Cell *120*, 649–661.

Kanety, H., Feinstein, R., Papa, M. Z., Hemi, R., and Karasik, A. (1995). Tumor necrosis factor alpha-induced phosphorylation of insulin receptor substrate-1 (IRS-1). Possible mechanism for suppression of insulin- stimulated tyrosine phosphorylation of IRS-1. J. Biol. Chem. *270*, 23780–23784.

Kops, G.J.P.L., Dansen, T. B., Polderman, P. E., Saarloos, I., Wirtz, K.W.A., Coffer, P. J., Huang, T. T., Bos, J. L., Medema, R. H., and Burgering, B.M.T. (2002). Forkhead transcription factor FOXO3a protects quiescent cells from oxidative stress. Nature *419*, 316–321.

Lee, S. R., Yang, K. S., Kwon, J., Lee, C., Jeong, W., and Rhee, S. G. (2002). Reversible inactivation of the tumor suppressor PTEN by $H_2O_2$. J. Biol. Chem. *277*, 20336–20342.

Lehtinen, M. K. *et al.* (2006). A conserved MST-FOXO signaling pathway mediates oxidative-stress responses and extends life span. Cell *125*, 987–1001.

Leslie, N. R. (2006). The redox regulation of PI 3-kinase-dependent signaling. Antioxid. Redox. Signal. *8*, 1765–1774.

Mahadev, K., Wu, X., Zilbering, A., Zhu, L., Lawrence, J. T., and Goldstein, B. J. (2001). Hydrogen peroxide generated during cellular insulin stimulation is integral to activation of the distal insulin signaling cascade in 3T3–L1 adipocytes. J. Biol. Chem. *276*, 48662–48669.

Migliaccio, E., Giorgio, M., Mele, S., Pelicci, G., Reboldi, P., Pandolfi, P. P., Lanfrancone, L., and Pelicci, P. G. (1999). The p66shc adaptor protein controls oxidative stress response and life span in mammals. Nature *402*, 309–313.

Park, H. S., Kim, M. S., Huh, S. H., Park, J., Chung, J., Kang, S. S., and Choi, E. J. (2002). Akt (protein kinase B) negatively regulates SEK1 by means of protein phosphorylation. J. Biol. Chem. *277*, 2573–2578.

Sonntag, W. E., Bennett, C., Ingram, R., Donahue, A., Ingraham, J., Chen, H., Moore, T., Brunso-Bechtold, J. K., and Riddle, D. (2006). Growth hormone and IGF-I modulate local cerebral glucose utilization and ATP levels in a model of adult-onset growth hormone deficiency. Am. J. Physiol. Endocrinol. Metab. *291*, E604–E610.

St-Pierre, J. *et al.* (2006). Suppression of reactive oxygen species and neurodegeneration by the PGC-1 transcriptional coactivators. Cell *127*, 397–408.

Taylor, J. M., Ali, U., Iannello, R. C., Hertzog, P., and Crack, P. J. (2005). Diminished Akt phosphorylation in neurons lacking glutathione peroxidase-1 (Gpx1) leads to increased susceptibility to oxidative stress-induced cell death. J. Neurochem. *92*, 283–293.

Torres-Aleman, I. (2005). Role of insulin-like growth factors in neuronal plasticity and neuroprotection. Adv. Exp. Med. Biol. *567*, 243–258.

Trejo, J. L., Carro, E., Garcia-Galloway, E., and Torres-Aleman, I. (2004). Role of insulin-like growth factor I signaling in neurodegenerative diseases. J. Mol. Med. *82*, 156–162.

van der Horst, A., and Burgering, B. M. (2007). Stressing the role of FoxO proteins in lifespan and disease. Nat. Rev. Mol. Cell Biol. *8*, 440–450.

Venters, H. D., Tang, Q., Liu, Q., VanHoy, R. W., Dantzer, R., and Kelley, K. W. (1999). A new mechanism of neurodegeneration: a proinflammatory cytokine inhibits receptor signaling by a survival peptide. Proc. Natl. Acad. Sci. USA *96*, 9879–9884.

Wu, D. C., Re, D. B., Nagai, M., Ischiropoulos, H., and Przedborski, S. (2006). The inflammatory NADPH oxidase enzyme modulates motor neuron degeneration in amyotrophic lateral sclerosis mice. Proc. Natl. Acad. Sci USA *103*, 12132–12137.

Zhong, J. and Lee, W. H. (2007). Hydrogen peroxide attenuates insulin-like growth factor-1 neuroprotective effect, prevented by minocycline. Neurochem. Int. *51*, 398–404.